Electronic Supplementary Material (ESI) for Journal of Materials Chemistry C.

Supporting information

Contrasting Analog and Digital Resistive Switching Memory Characteristics in Solution-Processed Copper (I) Thiocyanate and Its Polymer Electrolyte Based Memristive Devices

Rajesh Deb[a], Manjula G. Nair[b], Ujjal Das[c] and Saumya R. Mohapatra[a]*

[a]Department of Physics, National Institute of Technology Silchar, Silchar-788010, Assam, India

[b]Department of Physics, Indian Institute of Technology, Patna, Bihar, India, 801106

[c]Quantum Materials and Device Unit, Institute of Nano Science and Technology, Mohali-140306, Punjab, India

*Email:saumya@phy.nits.ac.in

Thickness measurement of CuSCN film by variable-angle spectroscopic ellipsometry (SE)

The thicknesses of the CuSCN films were measured using variable-angle spectroscopic ellipsometry (SE). Fig. 1 (a), (b), and (c) represent the measured SE parameters, such as psi (ψ) and delta (Δ) values, of CuSCN films deposited on glass substrates at 3000, 4000, and 5000 rpm by varying angles of 60°, 65°, and 70°. The fitted curves matched the experimental data well. The mean squared errors (MSE) of the CuSCN films spin-coated at 3000, 4000, and 5000 rpm were 3.167, 6.175, and 7.914, respectively. The low MSE values (<10) indicate a good fit with the experimental data. The thicknesses of the CuSCN films spin-coated at 3000, 4000, and 5000 rpm were approximately 168, 120, and 90 nm, respectively.

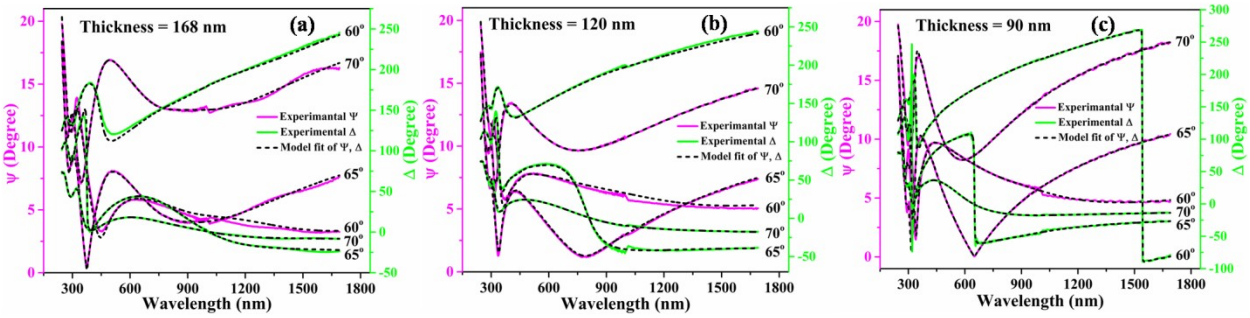

Figure S1. Variable angle spectroscopic ellipsometry of CuSCN films on glass substrate spin coated at (a) 3000 rpm, (b) 4000 rpm, (c) 5000 rpm. The solid magenta colour and green colour represents measured psi (ψ) and delta (Δ) spectra. The black dash represent the fitting of psi (ψ) and delta (Δ) spectra.

Characterization of Cu-SPE

Cross-sectional SEM

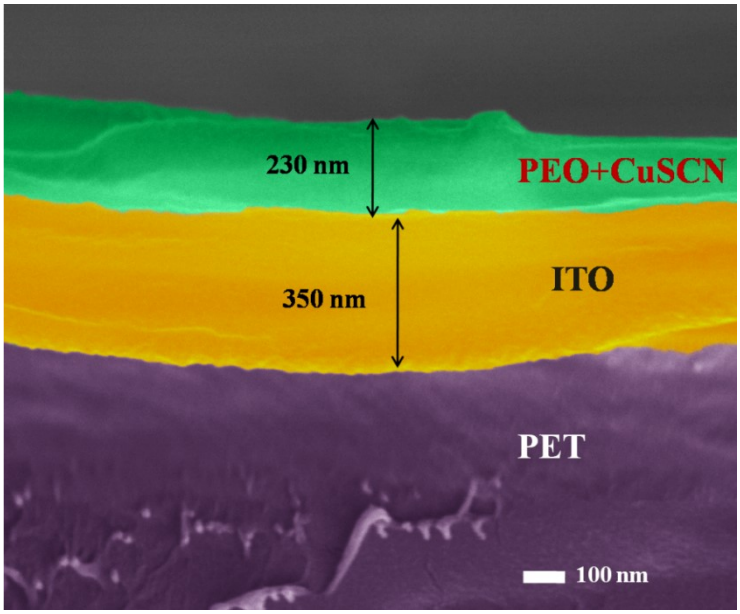

Figure S2. Cross-sectional SEM image of Cu-SPE layer deposited over ITO-coated PET substrate at 3000 rpm.

XRD and FTIR

The X-ray diffraction pattern of the copper ion conductive solid polymer electrolyte films with CUSCN (Cu-SPE) concentration of 0.25% to 5% is shown in Figure S3(a). The pattern shows two dominant peaks of PEO at 19.1° and 23.3°, which corresponds to (120) and (112) planes respectively.[1,2] It is observed that there is an increase in the intensity of (120) peaks with the rise in the salt concentration. This suggests that salt concentration has a strong influence on the crystallization process of the PEO. Further, no Bragg peak corresponding to CuSCN is observed in the electrolyte film, even at 5 wt.% of the CuSCN concentration. This indicates that no uncomplexed CuSCN is present in the electrolyte film. The FTIR spectra of the Cu-SPE film plotted as transmittance vs. wavenumber (580-3500 cm^{-1}) is shown in Figure S3(b). It confirms the characteristic vibrational modes of PEO in the wavenumber region 800-3000 cm^{-1}. The bands at 841cm^{-1} and 946 cm^{-1} are due to CH_2 asymmetric rocking motion with some contribution of C-O stretching. The sharp band at 1094 cm^{-1} is assigned to the C-O-C stretching mode. The relatively small bands at 1279 cm^{-1}, 1343 cm^{-1}, and 1463 cm^{-1} are because of CH_2 twisting, CH_2 wagging, and CH_2 deformation, respectively. The absorption band located at 2880 cm^{-1} is assigned to the C-H asymmetric stretching mode.[3,4] The C-N stretching band found at 2168 cm^{-1} was visible for higher concentrations of copper (I) thiocyanate salt.

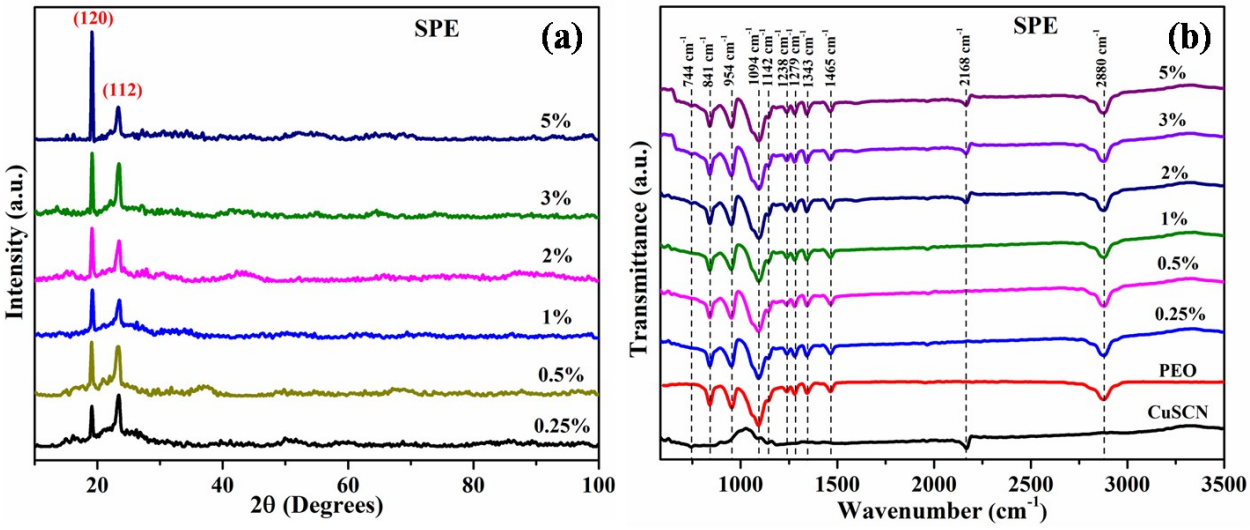

Figure S3. (a) X-ray diffraction pattern of Cu-SPE films, (b) FTIR spectra of Cu-SPE film in the wavenumber region 580-3500 cm^{-1}.

X-ray Photoelectron Spectroscopy (XPS)

The chemical and electronic state of atoms in the electrolyte film was investigated by X-ray photoelectron spectroscopy (XPS). The XPS full scan spectrum as shown in Fig. 10 (a), indicates the presence of Cu, S, C, N, and O in the film. The high-resolution spectrums of the S 2p, C 1s, N 1s, O 1s, and Cu 2p are shown in Fig. S4 (b)-(f). In the S 2p core level spectra, the component peak observed at binding energy (BE) of 162.2 eV is due to either C-S or Cu-S. The other two peaks at 163.8 eV and 168.8 eV correspond to S-C≡N and S-O environments. The C 1s core level spectra is dominated by a peak at 285.9 eV, which corresponds to CuSCN (S-C≡N), and the peak at 284.4 eV is due to the C-H environments of PEO. N 1s spectra show a dominant peak of CuSCN at 398.6 eV, and a small peak at 400.3 eV is due to the N-H environment. The O 1s spectrum of the electrolyte film consists of one peak at 532.3 eV, assigned as C-O-C. From the high-resolution spectra of the Cu 2p core levels, the peaks at 932 eV and 951.8 eV correspond to the prominent peaks of Cu $2p_{3/2}$ and Cu $2p_{1/2}$, respectively. The component peak at 933.1 eV is

due to the presence of Cu^{+} in the electrolyte film.[5-10] These sources indicate that the copper (I) thiocyanate separated into Cu^{+} and SCN^{-} ions in the polymer electrolyte.

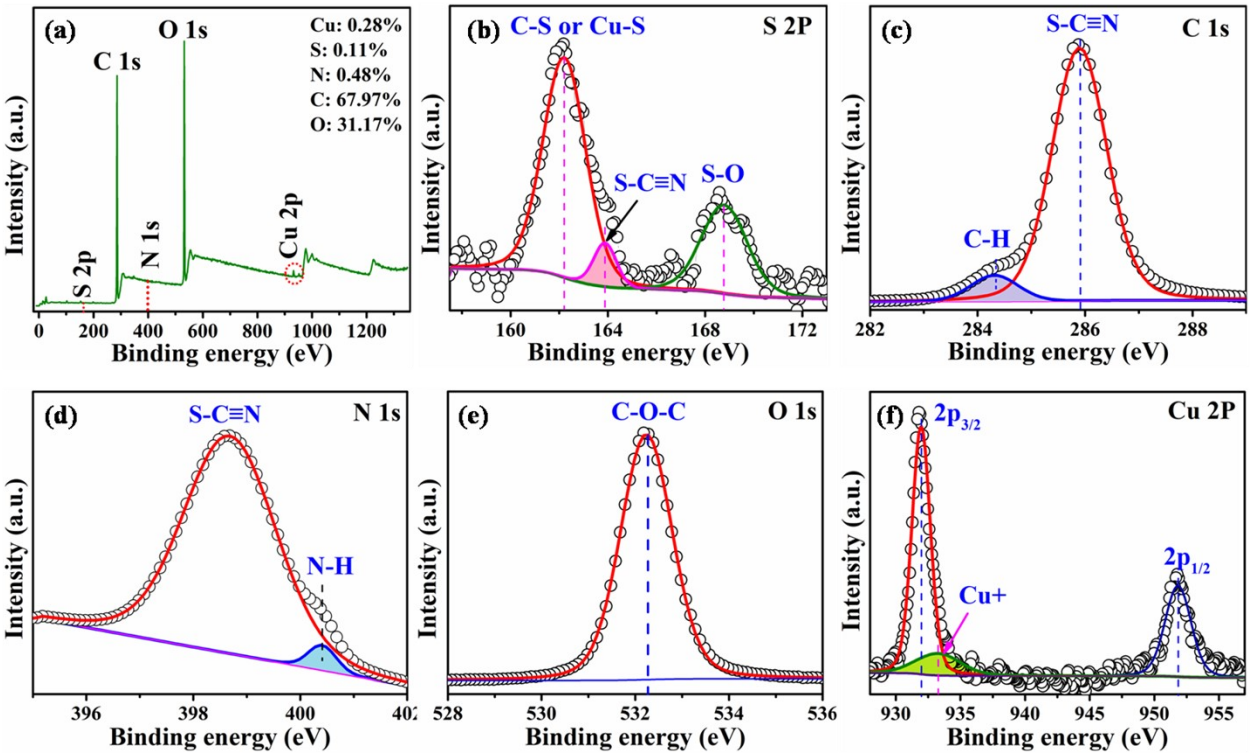

Figure S4. (a) XPS survey spectrum of the Cu-SPE film for 1 wt% of CuSCN. (b)-(f) High resolution spectra of the S 2p, C 1s, N 1s, O 1s and Cu 2p regions of the Cu-SPE film.

Current-Voltage characterstics of Cu/CuSCN/ITO memristive device spin-coated at 3000 rpm (~ 168 thick)

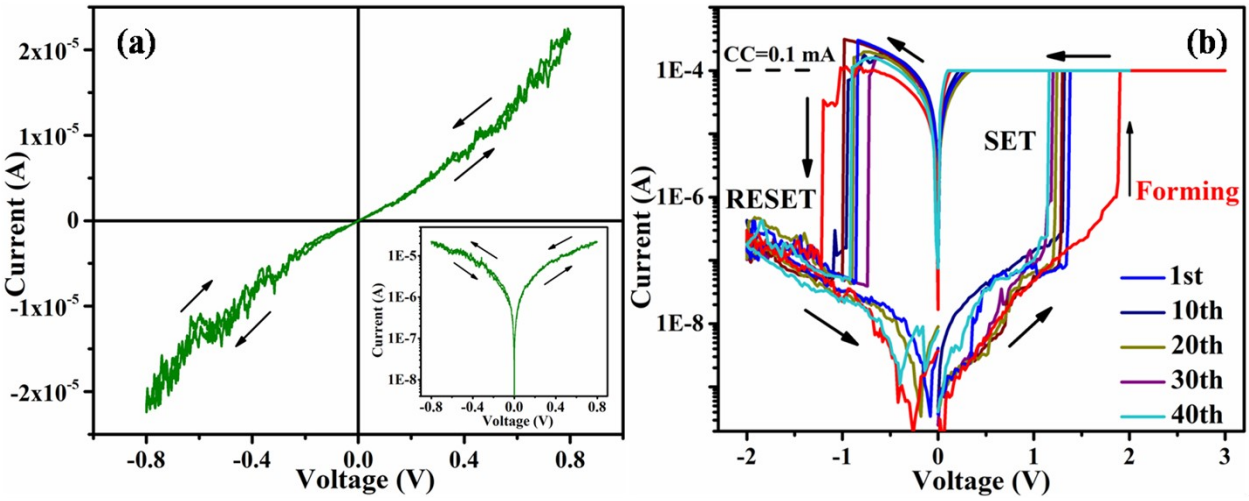

Figure S5. (a) Current-voltage characteristics of the Cu/CuSCN/ITO memristive device spin-coated at 3000 rpm. Inset of (a) represents the semi-logarithimic plot. (b) Bipolar *I-V* curves of Cu/CuSCN/ITO memristive cell spin coated at 3000 rpm.

Current-voltage characteristics of Au/CuSCN/ITO memristive device spin-coated at 4000 rpm

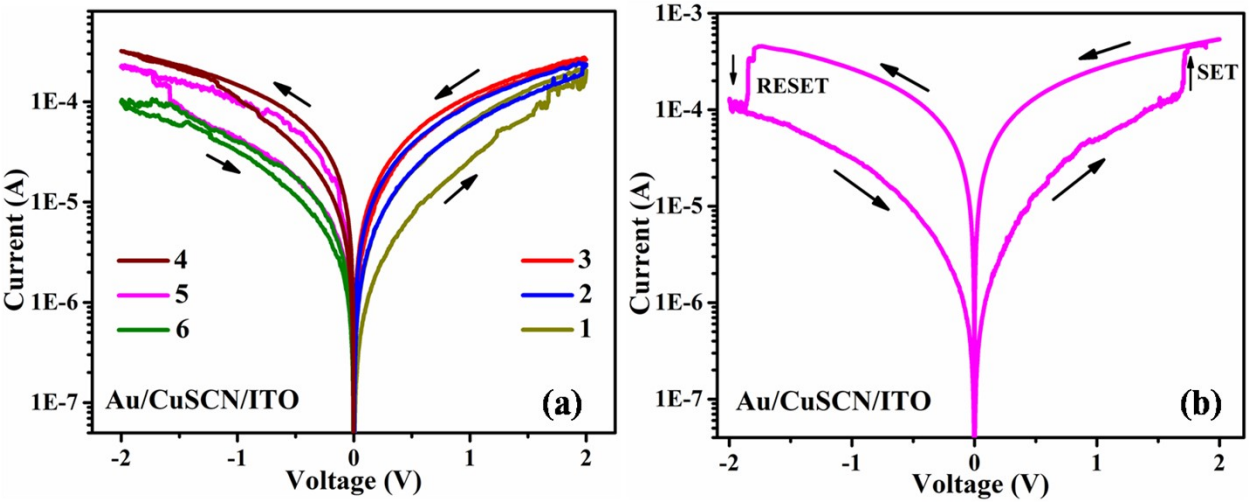

Figure S6. (a) Current-voltage characteristics of Au/CuSCN/ITO memristive device, where 1, 2, 3 represents the *I-V* curves under consecutive three positive voltage sweeps (0V → 2V → 0V) and 4, 5, 6 represents *I-V* curves under consecutive three negative voltage sweeps (0V → – 2V → 0V), respectively (b) Bipolar digital resistive switching as observed from the *I-V* characteristics in the Au/CuSCN/ITO memristive device.

Current-voltage (*I-V*) characteristics of Au/SPE/ITO memory device

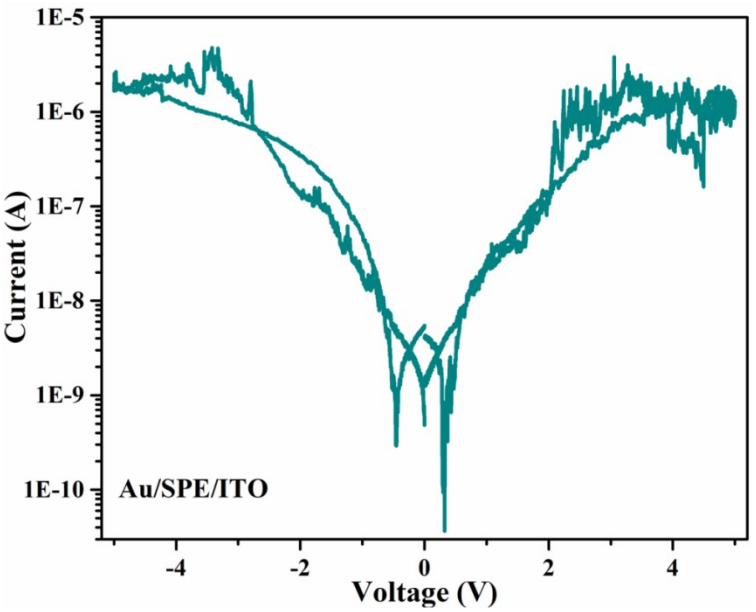

Figure S7. Current-voltage (*I-V*) characteristics of Au/SPE/ITO memory device.

REFERENCES

1 K. S. Sidhu, S. S. Sekhon, S. A. Hashmi and S. Chandra, *Eur. Polym. J.*, 1993, **29**, 779-782.
2 X. Xu, L. Jiang, Z. Zhou, X. Wu and Y. Wang, *ACS Appl. Mater. Interfaces*, 2012, **4**, 4331-4337.
3 S. R. Mohapatra, A. K. Thakur and R. N. P. Choudhary, *Journal of Polymer Science: Part B: Polymer Physics*, 2009, **47**, 60–71.
4 K. Sundaramahalingam, D. Vanitha, N. Nallamuthu, A. Manikandan and M. Muthuvinayagam, *Physica B: Condensed Matter*, 2019, **553**, 120-126.
5 N. Wijeyasinghe, A. Regoutz, F. Eisner, T. Du, L. Tsetseris, Y. H. Lin, H. Faber, P. Pattanasattayavong, J. Li, F. Yan, M. A. McLachlan, D. J.; Payne, M. Heeney and T. D. Anthopoulos, *Adv. Funct. Mater.*, 2017, 1701818.
6 J. E. Jaffe, T. C. Kaspar, T. C. Droubay, T. Varga, M. E. Bowden and G. J. Exarhos, *J. Phys. Chem. C*, 2010, **114**, 9111–9117.
7 B. Wang, S. Nam, S. Limbu, J. S. Kim, M. Riede and D. D. C. Bradley, *Adv. Electron. Mater.*, 2022, 2101253.
8 Q. Zhang, Y. Lu, H. Yu, G. Yang, Q. Liu, Z. Wang, L. Chen and Y. S. Hu, *Journal of the Electrochemical Society*, 2020, 167, 070523.
9 D. M. Vosshage and B. V. R. Chowdari, *J. Electrochem. Soc.*, 1995, **142**, 1442-1446.
10 U. Er, K. C. Icli and M. Ozenbas, *Journal of Solid State Electrochemistry*, 2020, **24**, 293–304.